Urol Res (2005) 33: 23–30
DOI 10.1007/s00240-003-0371-9

ORIGINAL PAPER

J. J. M. Pel · E. van Asselt · R. van Mastrigt

Contractile properties of inner and outer smooth muscle bundles from pig urinary detrusor

Received: 8 May 2003 / Accepted: 2 September 2003 / Published online: 22 January 2005

Abstract Like in the human detrusor, the pig urinary detrusor muscle consists of two layers: compactly arranged smooth muscle bundles on the mucosal side (inner layer) and loosely arranged smooth muscle bundles on the serosal side (outer layer). The contractile properties of muscle bundles of both layers were measured using the stop test followed by an isometric contraction. Total and passive forces were measured in ten muscle bundles from the inner and outer muscle layers. Active force was defined as the difference between total and passive force. The curvature and the unloaded shortening velocity of the force-velocity relation were calculated from the shortening forces measured during the stop test. The rate of force development was calculated from the isometric contraction. Differences in contractile properties between both layers were pairwise tested using the Wilcoxon Signed Ranks test. Percentage wise, the outer layer muscle bundles produced the highest active isometric force. The shortening forces were also higher in the outer layer bundles. As a result, both the curvature and the unloaded shortening velocity, derived from the average force-velocity relations fitted to the data sets, were higher in the muscle bundles from this layer. Finally, the outer layer muscle bundles contracted significantly faster than those of the inner layer. Muscle bundles from the outer layer of pig detrusor were found to be faster and stronger (more phasic) than the weaker and slower (more tonic) bundles from the inner layer, suggesting that during bladder contraction the outer layer of the detrusor does more work than the inner layer.

J. J. M. Pel (✉) · E. van Asselt · R. van Mastrigt
Department of Urology, sector Furore,
Erasmus MC, room EE 1630, PO Box 1738,
3000 DR Rotterdam, The Netherlands
E-mail: j.pel@erasmusmc.nl
Tel.: +31-10-4087377
Fax: +31-10-4089451

Keywords Smooth muscle · Contractility · Urinary bladder · Stop test · Pig

Introduction

Smooth muscle consists of long, spindle shaped cells that are interlaced. In most hollow organs, like the urinary bladder and the urethra, these cells are arranged in layers with different orientations [1]. In the last decade, studies have been published in which the properties of different smooth muscle organ layers were related to their function. For example, in female rabbit urethra tonic contractions were found in the circular muscle layer during bladder filling, whereas the longitudinal phasic muscle layer was active in opening the urethra before voiding [2]. In pig [3] and human [4] urethra, different smooth muscle layers (longitudinal and circular orientation) have been described also and it is thought that these layers play an active role in generating urethral pressure [5]. In human [6] and foetal bovine bladder [7] it was shown that the lamina propria acts as a capacitance layer, while the detrusor muscle prevents over-stretching of the bladder wall.

On the basis of magnetic resonance (MR) images compared with histological preparations, it was shown that pig [8] and human [8, 9, 10] bladder wall are of similar composition and that both consist of urothelium (~0.1 mm), lamina propria (~0.3 mm) and, surprisingly, an inner and an outer tunica muscularis (~3 mm total thickness) [9]. It was argued that it is not the arrangement of the muscle bundles but rather the more prominent presence of loose collagen bundles, blood vessels and water in the extracellular space of the outer muscle layer that causes differences in MR signal intensity [9]. In the present study, we measured the contractile properties of muscle bundles from the two different muscle layers in pig urinary bladder. The muscle lengths were kept within the physiological working range of the detrusor. We used the stop test to

measure the unloaded shortening velocity and an isometric contraction to measure the rate of force development.

Material and methods

Tissue handling: preparation and stimulation

Eight urinary bladders of freshly killed pigs (age: ~half a year; weight: 40–60 kg) were collected from the local slaughterhouse and transported in cold modified Krebs solution (118 mM NaCl; 4.7 mM KCl; 25 mM $NaHCO_3$; 1.2 mM KH_2PO_4; 1.8 mM $CaCl_2$; 1.2 mM $MgSO_4$ and 11 mM glucose aerated with 95% O_2 and 5% CO_2 (pH of 7.4)). Two strips of about 20×20 mm were cut from the antero-lateral wall of each bladder. One strip was kept overnight in 4°C Krebs solution for measurements the next day. Two small smooth muscle bundles were carefully cut from the other strip. Care was taken to cut bundles not wider than 0.7 mm in diameter using a binocular microscope and a fine ruler on the bottom of the preparation dish. One bundle was dissected just beneath the serosa and one was taken from the detrusor after removing the urothelium and tunica propria on the mucosal side. The bundles were studied in random order by clamping them between two pairs of tweezers in an organ bath. The first pair was connected to a length controller [11] and the second pair to a KG3 force transducer linked to a BAM3 amplifier (Scientific Instruments, Heidelberg, Germany). The muscle bundles were stimulated using an electrical field generated between two platinum electrodes. The signal applied to the electrodes was biphasic, 8 V in amplitude with a 125-Hz stimulation frequency and 5-ms pulse width. Previously, these stimulation parameters had been optimised in muscle bundles taken from the inner layer [11]. The temperature of the Krebs was kept at 37°C by infrared radiation.

Measurement protocol

Before attachment to the tweezers, the incubated bundles were electrically stimulated to attain the smallest physiological length. After a rest period of 10 min, the bundles were gently stretched to slack length (l_{slack}) defined by a passive force of ~150 μN in response to a small length increase. Then, the muscle bundles were stretched to a fixed stop length (l_{stop}), which was set at 200% of slack length ($l_{stop} = 2 * l_{slack}$). This stop length is below the length at which the highest isometric force would be measured, but is within the physiological working range of detrusor smooth muscle [11]. After two isometric test stimulations with 10-min interval time, the clamped bundle was slowly stretched to a start length (l_{start}). For example, to allow subsequent shortening for 4 s at a velocity of 50 μm/s, $l_{start} = l_{stop} + 4{\times}50$ μm. After 1 min, the muscle was shortened from l_{start} to l_{stop} at a pre-set velocity (v_{short}), first without stimulation to measure passive force (F_{pas}). Next, after restretching the muscle bundle to l_{start}, the stop test was repeated with the stimulation switched on to measure the total force (F_{tot}). Figure 1 shows the two force responses superimposed. The total force at l_{start} increased to a maximum value ($F_{tot.max}$). During shortening of the muscle bundles, F_{tot} decreased to a minimum value ($F_{tot.min}$) and recovered at l_{stop} to a second maximum ($F_{tot.rec}$). All total force values were corrected for the corresponding passive force values to derive the active force (F_{act}). After another 5-min waiting time, an isometric contraction at l_{stop} was measured (see Fig. 2). The maximum total isometric force ($F_{iso.tot.max}$) was compared to the force value at cessation of the stimulation ($F_{iso.tot.end}$). With 10-min rest intervals, the stop test was repeated using five different shortening velocities in the following order: v_{short} = 25, 100, 75, 175 and 50 μm/s with a shortening duration of 4 s. This resulted in five different length changes superimposed on l_{stop}: 100, 400, 350, 700 and 200 μm.

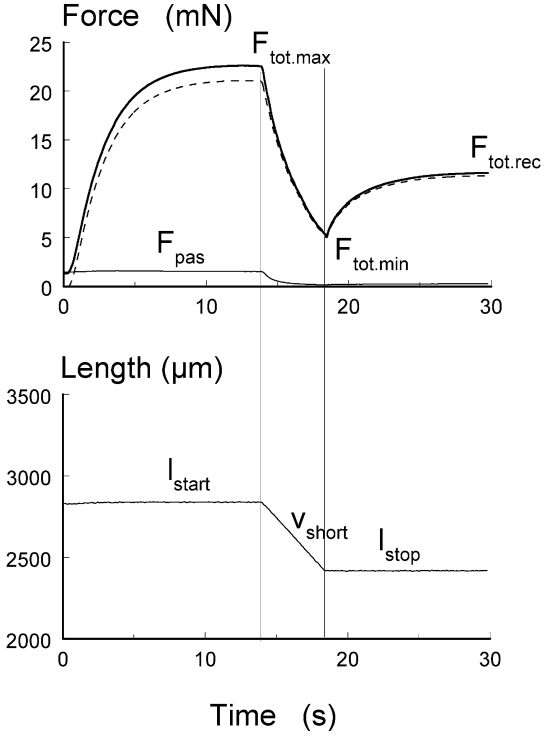

Fig. 1 An example of a stop test measurement. First, a measurement was done without stimulation to measure the passive force (F_{pas}). Then, with stimulation, the total force (F_{tot}) was measured. Both measurements are presented superimposed. Upon stimulation, the total force in the upper panel increased to a maximum value ($F_{tot.max}$). Then, the muscle bundle was shortened from start length (l_{start}) to stop length (l_{stop}) at a pre-set shortening velocity (v_{short}). F_{tot} decreased to a minimum ($F_{tot.min}$) during shortening. Afterwards, it recovered to an isometric value ($F_{tot.rec}$). The *dotted line* is the difference between the total force and the passive force and was denoted as active force (F_{act})

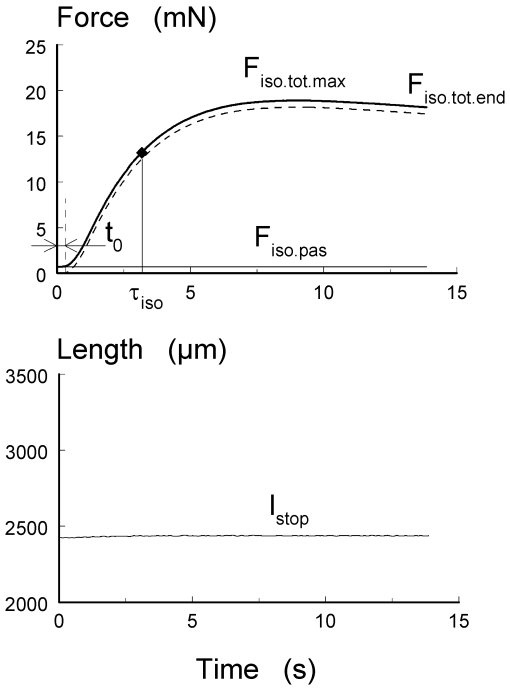

Fig. 2 An example of an isometric force measurement. The preceding stop test in this muscle bundle is shown in Fig. 1. The muscle bundle was kept at stop length (l_{stop}). Passive force ($F_{iso.pas}$) was measured without stimulation. Upon stimulation, the total isometric force ($F_{iso.tot}$) increased to a maximum ($F_{iso.tot.max}$) and the force at the end of the stimulation was denoted as ($F_{iso.tot.end}$). A mono-exponential equation was fitted to the total isometric force curve to calculate the time constant (τ_{iso}) and the delay time (t_0) between activation of the stimulation field and force generation. The *dotted line* represents the active force (F_{act}), which was calculated as the difference between the isometric and passive force

Data processing

All measurements were analysed using self-written programs (Matlab). To normalise the forces, we divided the forces measured during the stop test by those measured during the subsequent isometric contraction. Thus, in each bundle, the normalised total force ($\overline{F_{tot.max}}$) and normalised passive force ($\overline{F_{pas}}$) were calculated as $\frac{F_{tot.max}}{F_{iso.tot.max}}$ and $\frac{F_{pas}}{F_{iso.pas}}$, respectively. The normalised maximum active force ($\overline{F_{act.max}}$) was derived as $\frac{F_{tot.max}-F_{pas}}{F_{iso.tot.max}-F_{iso.pas}}$. In addition, the percentage of passive force at l_{start} ($\%F_{pas}$) and the percentage of passive isometric force at l_{stop} ($\%F_{iso.pas}$) were derived as the quotient $100\% \cdot \left(\frac{F_{pas}}{F_{tot.max}}\right) 100\% \cdot \left(\frac{F_{iso.pas}}{F_{iso.tot.max}}\right)$.

The corresponding percentage active force at l_{start} ($\%F_{act.max}$) and that at l_{stop} ($\%F_{iso.act.max}$) were derived as 100%-$\%F_{pas}$ and 100%-$\%F_{iso.pas}$, respectively. All quotients were plotted against the corresponding normalised muscle bundle length $\frac{l_{start}-l_{stop}}{l_{stop}}$ and a second order polynomial was fitted to the complete data set of inner and outer layer smooth muscle bundles. To derive a force-velocity relation, we plotted the relative force (F_{rel}), defined as the quotient of $F_{act.min}$ and $F_{act.rec}$ against the normalised shortening velocity (v_{short}/l_{stop}). A hyperbolic (Hill) force-velocity was rewritten in terms of three independent parameters [12]: the maximum of the relative force (F/F_0), the curvature of the force-velocity relation (a/F_0) and the normalised unloaded shortening velocity ($v_{short.max}/l_{stop}$). While fixing the maximum of the relative force at 1, a/F_0 and $v_{short.max}/l_{stop}$ were optimised using a least square fitting procedure. It was found that most of the variation in the force and velocity data pairs was expressed in a/F_0. Therefore, we also optimised a one-parameter model, varying $v_{short.max}/l_{stop}$ only. In this case, not only the relative force was fixed at 1 but also the curvature was fixed at the value of the average curvature derived from both the outer and inner layer muscle bundles.

A mono-exponential curve was fitted to all isometric contractions to calculate the time constant (τ_{iso}) (see Fig. 2). A delay time (t_0) between activation of the stimulation field and onset of force generation was accounted for. To quantify force maintenance during the isometric contraction, we calculated the difference between the maximum isometric force and the isometric force at the end of stimulation $\frac{F_{iso.tot.max}-F_{iso.tot.end}}{F_{iso.tot.end}}$.

The differences in force values and time constants between the inner and outer layer of each bladder were pairwise tested for significance using a Wilcoxon Signed Ranks test (SPSS). Analysis of variance was applied to test the effect of bladder number and freshness (i.e. fresh and one-day-old bladder) on the parameters τ_{iso}, $\%F_{iso.pas}$ and $\%F_{iso.act.max}$. The definitions of all calculated parameters are summarised in Table 1.

Results

Fresh and 1-day-old muscle bundles were cut from three detrusors (six outer and six inner bundles). From two more detrusors we only cut fresh bundles (two outer and two inner bundles); from three others, we only processed bundles the day after excision (three outer and three inner bundles). One outer and one inner bundle of the same bladder died because the circulation of fresh Krebs to the organ bath failed. Thus in total, ten inner and ten outer muscle bundles were pairwise studied. Figure 3 shows the normalised force-length relation, representing $\overline{F_{tot.max}}$ (*top panel*) $\overline{F_{pas}}$ (*middle panel*) and $\overline{F_{act.max}}$ (*lowest panel*) measured in outer (*closed triangles*) and inner (*open triangles*) layer muscle bundles. With increasing muscle length, $\overline{F_{tot.max}}$ and $\overline{F_{pas}}$ increased most in the inner layer bundles. $\overline{F_{act.max}}$, however, did not differ between both layers. The second order polynomials fitted to $\overline{F_{act.max}}$ showed a rising tendency, indicating that all stop test measurements were done at start lengths below the length at which the active force is highest, thus below the optimum length. In Fig. 4, the $\%F_{pas}$ (*upper panel*) and the $\%F_{act.max}$ (*lowest panel*) of $F_{tot.max}$ are plotted against

Table 1 A summary of all definitions of the calculated parameters

Parameter:	Definition:
$\overline{F_{tot.max}} = \frac{F_{tot.max}}{F_{iso.tot.max}}$	Normalised total force
$\overline{F_{pas}} = \frac{F_{pas}}{F_{iso.pas}}$	Normalised passive force
$\overline{F_{act.max}} = \frac{F_{tot.max} - F_{pas}}{F_{iso.tot.max} - F_{iso.pas}}$	Normalised active force
$\%F_{pas} = 100\% \cdot \left(\frac{F_{pas}}{F_{tot.max}}\right)$	Percentage passive of total force
$\%F_{act.max} = 100\%\text{-}\%F_{pas}$	Percentage active of total force
$\%F_{iso.pas} = 100\% \cdot \left(\frac{F_{iso.pas}}{F_{iso.tot.max}}\right)$	Percentage passive of isometric force
$\%F_{iso.act.max} = 100\%\text{-}\%F_{iso.pas}$	Percentage active of isometric force
$\frac{l_{start} - l_{stop}}{l_{stop}}$	Normalised muscle bundle length
$F_{rel} = \frac{F_{act.min}}{F_{act.rec}}$	Relative (shortening) force
v_{short}/l_{stop}	Normalised shortening velocity
F/F_0	Maximum shortening force
a/F_0	Curvature
$v_{short.max}/l_{stop}$	Normalised unloaded shortening velocity
$\frac{F_{iso.tot.max} - F_{iso.tot.cal}}{F_{iso.tot.cal}}$	Force maintenance

the normalised length. Percentage wise, the outer layer muscle bundles produced the highest active force and the inner layer bundles the highest passive force.

Table 2 summarises the contractile properties derived from the stop test for both layers. The F_{rel} values of the muscle bundles in the outer layer muscle were significantly higher than those in the inner layer. To determine the force-velocity relation, we plotted the F_{rel} against v_{short}/l_{stop} of outer and inner layer muscle bundles and fitted a hyperbolic force-velocity relation to both data sets (see Fig. 5). First, a/F_0 and $v_{short.max}/l_{stop}$ were both optimised. We then found that a/F_0 was two times higher for the outer layer compared to the inner layer (0.32 versus 0.15). To optimise only the unloaded shortening velocity, the curvature was fixed at the average value for both layers of 0.24. We derived that $v_{short.max}/l_{stop}$ of the outer layer was higher than that of the inner layer (0.191 1/s versus 0.156 1/s). In Fig. 5, the average force-velocity relations derived for the outer and inner layer are shown. Note that for the presentation of both force-velocity relations, we fixed the curvature to the average value of both calculations; thus, for the outer layer bundles $a/F_0 = 0.28$ ((0.32 + 0.24)/2) and for the inner layer $a/F_0 = 0.19$ ((0.15 + 0.24)/2).

Table 3 summarises the properties derived for both layers from the isometric contractions. Pairwise testing of the time constant, τ_{iso}, showed that the isometric contraction developed significantly faster in the outer layer than in the inner layer. The delay time, t_0, was equal in both layers. Comparing $F_{iso.tot.max}$ with $F_{iso.tot.end}$ showed that the $F_{iso.tot.max}$ values in the inner layer remained at a plateau level (implying tonic contraction) and decreased in the outer layer (implying phasic contraction). Finally, the variation in bladders and in freshness did significantly influence τ_{iso} in both layers. We found that 1-day-old tissue contracted significantly faster (smaller time constant) than fresh tissue. In both layers, $\%F_{iso.pas}$ and $\%F_{iso.act.max}$ were not significantly different among the eight bladders and between fresh and 1-day-old tissue.

Discussion

The aim of this study was to measure the contractile properties of the two smooth muscle layers found in pig urinary bladder. The stop test was used to measure the unloaded shortening velocity of the smooth muscle bundles in the physiological working range of the bladder. It involves measurement of force generation of electrically stimulated muscle fibres during shortening from a pre-set start length to a fixed stop length at a pre-set shortening velocity. More often, the quick release method is used to measure the unloaded shortening velocity. One of the advantages of the quick release method is that the muscle bundles do not need to be 'over-stretched' to measure the shortening velocity at a pre-set muscle length. The stop test, on the other hand, has the advantage that the force related to a pre-set shortening velocity is measured at exactly the pre-set stop length. Most important, however, passive force can be measured and corrected for at this length, too. In smooth [14] and also striated [15] muscle physiology, such corrections for passive force contribute highly to the understanding of the mechanism of contracting muscle. Previously, the differences between electrically and pharmacologically stimulated pig urinary bladder strips were studied by means of isometric forces and time constants [13]. Compared to the isometric forces found in electrically stimulated muscle bundles, isometric force values were higher in potassium-stimulated contractions, lower in ATP-stimulated contractions and equal to acetylcholine-stimulated contractions. The time constants of the electrically stimulated contractions were faster than those calculated from pharmacologically stimulated contractions.

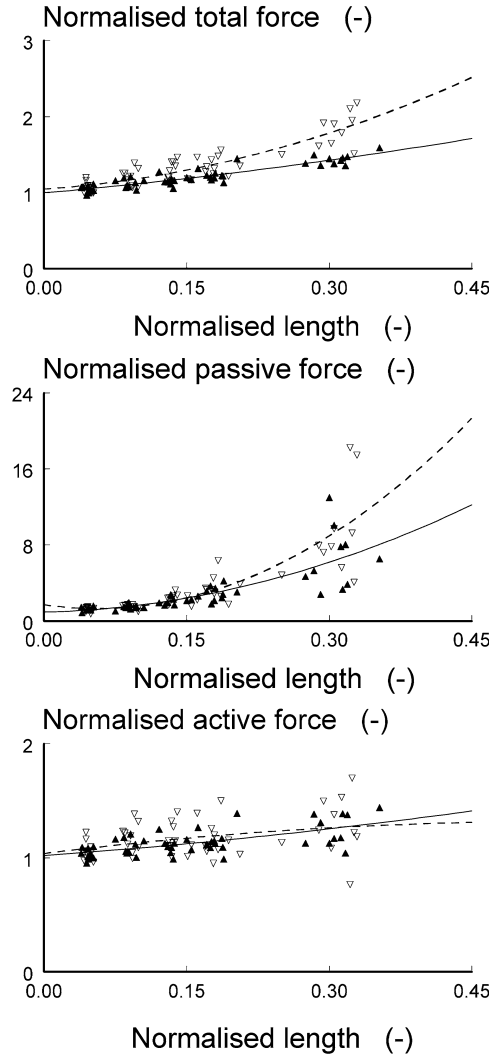

Fig. 3 The forces measured at start length (l_{start}) during the stop test were normalised by dividing by those measured during the isometric measurement at stop length (l_{stop}); see also Figs. 1 and 2. This figure shows the normalised force-length relations of the total force ($\overline{F_{tot.max}}$;*top panel*, passive force($\overline{F_{pas}}$;*middle panel*) and active force ($F_{act.max}$;*lowest panel*) against the normalised muscle lengths (l_{start}-l_{stop}/l_{stop}). A second order polynomial was fitted to the data set of outer (*closed triangles; straight line*) and inner (*open triangles; dotted line*) muscle bundles to visualise the tendency of the normalised force-length relation

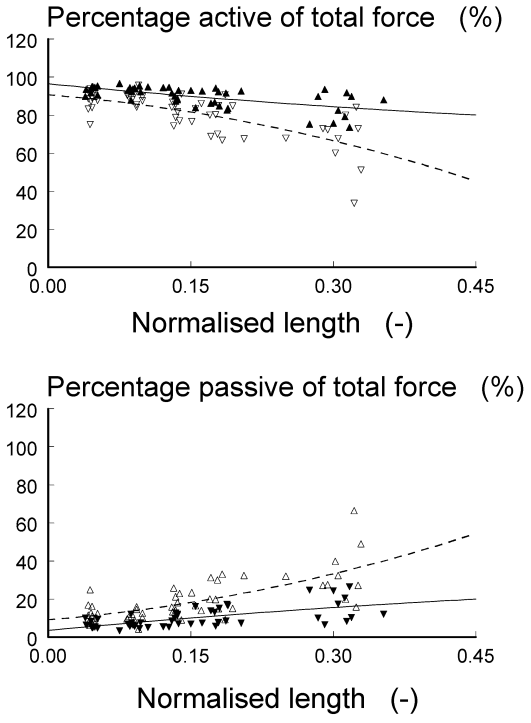

Fig. 4 The percentage active (*upper panel*) and passive (*lower panel*) force of the total force measured at start length in outer (*closed triangles*) and inner (*open triangles*) layer muscle bundles (*upper panel*) as a function of the normalised muscle length, derived from Fig. 1

In the present study, forces at different shortening velocities were measured at 200% of the slack length. We found that, percentage wise, the outer muscle layer produced the highest active isometric force. Our findings suggest that the differences in the ratio of muscle/connective tissue between outer and inner layer bundles of comparable size explain the differences in contractile properties. Histologic preparations from two pig bladders confirmed that the outer layer is well developed, showing thick muscle bundles (longitudinally orientated) that are loosely arranged and surrounded by relatively small amount of connective tissue (elastin, collagen) (see Fig. 6). In contrast, the inner layer consists mostly of small muscle bundles (circularly orientated) situated in a denser network of connective tissue. As mentioned, due to the loosely arranged muscle bundles in the outer layer, relatively more water and blood vessels are present in this layer, which was detected using MR technology. In the classic Hill model [15], connective tissue that encircles the muscle cells is symbolised by a parallel elastic element. This element may accumulate energy when it is stretched (it then acts as a passive spring) or compressed (it then resists an increasing cross sectional area of the muscle bundle). Thus, when a muscle bundle is actively shortened, part of the energy is accumulated by the connective tissue, which decelerates the contraction velocity of the muscle cells. Furthermore, the normalised unloaded shortening velocity was lowest in the inner layer, which could also be explained by a relatively high percentage of connective tissue between the muscle cells. Analysis of variance showed that variation in bladder and their freshness had no significant influence on the percentage of passive and active isometric force calculated from the isometric contraction. However, variation in bladder and their freshness did significantly influence the rate of force development, expressed by the time constant. Previously, it was shown in rat that ageing of the bladder of about 20 weeks did not affect force-generating capacity of longitudinal smooth muscle, but a decrease was found in muscarinic responsiveness [16, 17]. In addition, an increase in contractions evoked by electrical stimulation suggested a decrease in compliance caused by an increase in collagen in the circular detrusor

Table 2 Summarised results (mean ± 1 SD) of the stop test measurements in ten outer and ten inner layer pig detrusor smooth muscle bundles. Each muscle bundle was shortened at five different shortening velocities. The parameters were pairwise tested for significance (outer and inner bundles from the same detrusor) using the Wilcoxon Signed Ranks test

	Outer layer	Inner layer	*p* value
l_{stop}(μm)	2249 ± 147 (n = 50)	2202 ± 147 (n = 50)	$p = 0.196$
F_{rel}(−) at v = 25 μm/s	0.85 ± 0.05 (n = 10)	0.77 ± 0.05 (n = 10)	$p < 0.01$
F_{rel}(−) at v = 50 μm/s	0.62 ± 0.07 (n = 10)	0.54 ± 0.07 (n = 9)	$p < 0.05$
F_{rel}(−) at v = 75 μm/s	0.48 ± 0.07 (n = 10)	0.41 ± 0.04 (n = 10)	$p < 0.05$
F_{rel}(−) at v = 100 μm/s	0.39 ± 0.05 (n = 10)	0.33 ± 0.03 (n = 10)	$p < 0.01$
F_{rel}(−) at v = 175 μm/s	0.23 ± 0.05 (n = 10)	0.20 ± 0.02 (n = 9)	$p < 0.05$
$v_{short.max}/l_{stop}$(1/s)	0.191	0.156	-
T (C)	37.0 ± 0.1	36.9 ± 0.1	-

The relative forces (F_{rel}) were measured during shortening of the muscle bundles to a fixed length, the stop length (l_{stop}); see also Fig. 1. The normalised unloaded shortening velocity ($v_{short.max}/l_{stop}$) was derived by fitting a hyperbolic shaped curve to the relative forces measured at five different shortening velocities in outer and inner layer muscle bundle. The temperature (T) was kept at 37°C

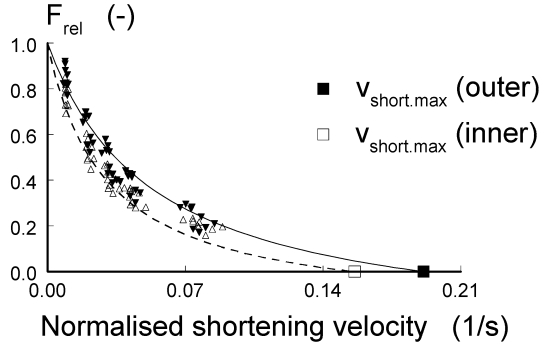

Fig. 5 The relative forces in outer (*closed triangles*) and inner (*open triangles*) layer muscle bundles are plotted against the normalised shortening velocity applied. The maximum unloaded shortening velocity of the outer layer bundles was 20% higher than that of the inner layer bundles

of aged rats [17]. The effect of ageing was found to be specific for different regions and functional components of the rat bladder, probably due to the changes in muscarinic receptors and collagen. It could be that storing pig bladder tissue for 24 h affected some of the metabolic properties. We think that the observed contractile changes may be ascribed to the reduced condition of passive elastic elements, e.g. collagen, as described in rat bladder [17]. When muscle becomes stiffer, it more resists the increase of the cross section area when it is stimulated to contract. In this more rigid state, maximum isometric force can be reached more quickly, since the contracting elements only contribute to force increase, hence a decrease of the time constant.

The passive and active properties of bladder smooth muscle have been studied extensively in small and large muscle strips to investigate the function of the organ involved. Mostly, the muscle strips were of full wall thickness and cut longitudinally from the base to the top of the organ or circularly, perpendicular to that direction. In rat bladder [17, 18] and guinea pig stomach [19, 20] contractile differences have been reported between muscle strips of both directions. Based on the presented findings we conclude that, in addition to orientation, the two different detrusor layers also vary in mechanical properties. The (human) bladder function can be (partly) described on the basis of the mechanical, pharmacological and contractile properties of the organ layers separately. It was shown that during filling of the bladder, the lamina propria acts as a capacitance layer [7]. The relative thickness of this layer decreases faster than the thickness of the detrusor. When the bladder is filled near capacity, the tension in the bladder wall is mainly generated by the detrusor muscle to prevent overstretching of the bladder wall. Our study shows that this passive tension exists predominantly in the inner layer of the detrusor muscle. Before voiding starts, the urethra relaxes and the detrusor is stimulated to reach the

Table 3 Summarised results (mean values ± 1 standard deviation) of the isometric contractions that followed each stop test in ten outer and ten inner layer pig detrusor smooth muscle bundles. The parameters were all measured at a fixed reference length, the stop length (l_{stop}), and pairwise tested for significance (outer and inner bundles from the same detrusor) using the Wilcoxon Signed Ranks test

	Outer layer	Inner layer	*p* value
τ_{iso}(s)	3.1 ± 0.7 (n = 48)	3.6 ± 0.7 (n = 50)	$p < 0.001$
t_0(s)	0.5 ± 0.1 (n = 49)	0.5 ± 0.1 (n = 50)	$p = 0.055$
$\frac{F_{iso.tot.max} - F_{iso.tot.calend}}{F_{iso.tot.cal}}$ (−)	0.06 ± 0.07 (n = 49)	0.02 ± 0.03 (n = 50)	$p < 0.001$
T (C)	37.0 ± 0.1	36.9 ± 0.1	-

To the isometric contraction, a mono-exponential curve was fitted to calculate the time constant of the contraction (τ_{iso}) and the delay time between activation of the stimulation field and the force generation in the muscle bundle (t_0). The maximum total isometric force ($F_{iso.tot.max}$) and the force at cessation of the stimulation ($F_{iso.tot.end}$) were compared. The temperature (T) was kept at 37°C

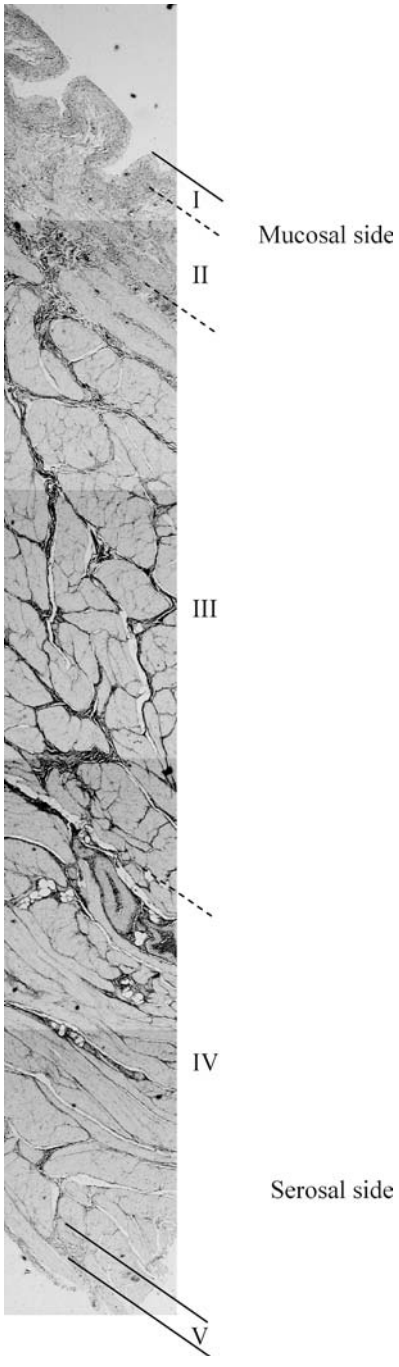

Fig. 6 Cross-section of the pig urinary detrusor (elastic von Gieson staining) showing muscle tissue surrounded by elastin/collagen fibres. Five different layers can be distinguished: (I) tunica mucosa, (II) tunica propria, (III) inner (or ventral) tunica muscularis, (IV) outer (or dorsal) tunica muscularis and tunica serosa (V). Note the differences in arrangement of the smooth muscle bundles of the loose, spacious outer tunica muscularis more or less perpendicular to those in the compact inner tunica muscularis. The inner layer appears to consist of relatively more connective tissue than the outer layer

opening pressure of the urethra. Our finding suggests that at the onset of voiding, the outer layer muscle fibres contribute most to the rise in bladder pressure. When the bladder pressure has reached the opening pressure, urine is pushed through the urethra to unfold it and voiding commences. The detrusor wall contracts at a certain shortening velocity to push the urine through the urethra and, based on the present results, the muscle fibres in the outer layer still produce the highest force. In addition, we found, by comparing the isometric force with the force at the end of the stimulation, that the relatively low isometric force remained longer at a plateau level in inner layer bundles than compared to outer layer bundles. Previously, it was shown that during voiding the tonal circular layers in the rabbit urethra relax, whereas phasic longitudinal layers contract to open up the urethra [2]. This finding may indicate that, analogous to urethra, the pig detrusor consists of a weaker contracting tonic (inner) and a stronger contracting phasic (outer) layer. However, the contractile differences we found between tonic inner and phasic outer detrusor muscle layers are not as pronounced as that found in rabbit urethra [2]. Additional histochemical tests need to be done to characterise further the muscle tissue in both layers. Since it was shown in female pig that the inner longitudinal smooth muscle layer of the urethra is continuous with the inner longitudinal layer of the detrusor [5], our findings suggest that similar differences of contractile properties found in the detrusor might also exist in layers of the female pig bladder neck and urethral smooth muscle.

Conclusions

It was previously shown that pig and human urinary bladder wall are similar in composition and contain an inner and an outer muscle layer. Presently, we found that the outer muscle layer contributes most to an isometric contraction. The weaker contracting inner layer maintains the contraction longer than the stronger outer layer, which suggests a tonic inner and a phasic outer layer. When the bladder wall contracts, the muscle fibres in the outer layer produce the highest force. We conclude that the outer layer of the detrusor does more work than the inner layer.

Acknowledgements This research was supported by the Technology Foundation STW, applied division of the Netherlands Organisation for Scientific Research (NWO) and the technology programme of the Ministry of Economic affairs. The authors thank Bas de Jong and Jojanneke Coppens for their help with the histological preparations.

References

1. Woodburne RT (1968) Anatomy of the bladder and bladder outlet. J Urol 100(4): 474–487
2. Arner A, Mattiasson A, Radzizewski P, Uvelius B (1998) Shortening velocity is different in longitudinal and circular muscle layers of the rabbit urethra. Urol Res 26(2): 423–426
3. Khanna OP, Barbieri EJ, Altamura M, McMicheal R (1981) Vesicourethral smooth muscle: function and relation to structure. Urology 18(2): 211–218

4. Brading AF, Teramoto N, Dass N, McCoy R (2001) Morphological and physiological characteristics of urethral circular and longitudinal smooth muscle. Scand J Urol Nephrol Suppl 207:12–18
5. Dass N, McMurray G, Greenland JE, Brading AF (2001) Morphological aspects of the female pig bladder neck and urethra: quantitative analysis using computer assisted 3-dimensional reconstructions. J Urol 165(4): 1294–1299
6. Ewalt DH, Howard PS, Blyth B, Snyder HM 3rd, Duckett JW, Levin RM, Macarak EJ (1992) Is lamina propria matrix responsible for normal bladder compliance? J Urol 148(2): 544–549
7. Chang SL, Chung JS, Yeng MK, Howard PS, Macarak EJ (1999) Roles of the lamina propria and the detrusor in tension transfer during bladder filling. Scand J Urol Nephrol Suppl 201:38–45
8. Teufl F, Dammann F, Wehrmann M (1997) In vitro study of morphology of the bladder wall using MR tomography at 1.0 Tesla: correlation with histology. Rofo Fortschr Geb Rontgenstr Neuen Bildgeb Verfahr 166(5): 406–410
9. Narumi Y, Kadota T, Inoue E, Kuriyama K, Horinouche T, Kasai K, Maeda H, Kuroda M, Kotake T, Ishiguro S (1993.) Bladder wall morphology: in vitro MR imaging-histopathologic correlation. Radiology 187:151–155,
10. Dixon JS, Gosling JA (1983) Histology and fine structure of the muscularis mucosae of the human urinary bladder. J Anat 136(2): 265–271
11. Minekus JP, van Mastrigt R (2001) Length dependence of the contractility of pig detrusor smooth muscle bundles. Urol Res 29(2): 126–133
12. van Mastrigt R (1980) Fitting the Hill equation to experimental data. IEEE transactions on biomedical engineering. Vol. BME 27(7): 412–416
13. van Koeveringe GA, van Mastrigt R (1991) Excitatory pathways in smooth muscle investigated by phase plot analysis of isometric force development. Am J Physiol 261(1): R138–R144
14. van Mastrigt R (2002) Mechanical properties of (urinary bladder) smooth muscle. J Muscle Res Cell Motil 23(1): 53–57
15. Hill AV (1938) The heat of shortening and the dynamic constants of muscle. Proc R Soc Lond B Biol Sci 126:136–195
16. Munro DD, Wendt IR (1993) Contractile and metabolic properties of longitudinal smooth muscle from rat urinary bladder and the effects of aging. J Urol 150:529–536
17. Pagala MK, Tetsoti L, Nagpal D, Wise GJ (2001) Aging effects on contractility of longitudinal and circular detrusor and trigone of rat bladder. J Urol 166(2): 721–727
18. Schroder A, Uvelius B, Capello SA, Longhurst PA (2002) Regional differences in bladder enlargement and in vitro contractility after outlet obstruction in the rabbit. J Urol 168(3): 1240–1246
19. Kuriyama H, Mishima K, Suzuki H (1975) Some differences in contractile response of isolated longitudinal and circular muscle from the guinea-pig stomach. J Physiol 251(2): 317–331
20. Moriya M, Miyazaki E (1985) Force-velocity characteristics of stomach muscle: a comparison between longitudinal and circular muscle strips. Comp Biochem Physiol A 81(3): 531–537
21. Watanabe H, Yamamoto TY (1979) Autonomic innervation of the muscles in the wall of the bladder and proximal urethra of male rats. J Anat 128(4): 873–886